

Isobutyl acetate: electronic state spectroscopy by high-resolution vacuum ultraviolet photoabsorption, He(I) photoelectron spectroscopy and ab initio calculations^{*}

Malgorzata A. Śmiałek^{1,2,a}, Marta Labuda³, Marie-Jeanne Hubin-Franskin⁴, Jacques Delwiche⁴, Søren Vrønning Hoffmann⁵, Nykola C. Jones⁵, Nigel J. Mason², and Paulo Limão-Vieira⁶

¹ Department of Control and Power Engineering, Faculty of Ocean Engineering and Ship Technology, Gdańsk University of Technology, Gabriela Narutowicza 11/12, 80-233 Gdańsk, Poland

² School of Physical Sciences, The Open University, Walton Hall, Milton Keynes MK7 6AA, UK

³ Department of Theoretical Physics and Quantum Information, Faculty of Applied Physics and Mathematics, Gdańsk University of Technology, Gabriela Narutowicza 11/12, 80-233 Gdańsk, Poland

⁴ Département de Chimie, Université de Liège, Institut de Chimie – Bât. B6C, 4000 Liège, Belgium

⁵ ISA, Department of Physics and Astronomy, Aarhus University, Ny Munkegade 120, 8000 Aarhus C, Denmark

⁶ Laboratório de Colisões Atômicas e Moleculares, CEFITEC, Departamento de Física, Faculdade de Ciências e Tecnologia, Universidade NOVA de Lisboa, 2829-516 Caparica, Portugal

Received 31 January 2017 / Received in final form 24 March 2017

Published online 25 May 2017

© The Author(s) 2017. This article is published with open access at Springerlink.com

Abstract. The high-resolution vacuum ultraviolet photoabsorption spectrum of isobutyl acetate, C₆H₁₂O₂, is presented here and was measured over the energy range 4.3–10.8 eV (290–115 nm). Valence and Rydberg transitions with their associated vibronic series have been observed in the photoabsorption spectrum and are assigned in accordance with new ab initio calculations of the vertical excitation energies and oscillator strengths. The measured photoabsorption cross sections have been used to calculate the photolysis lifetime of this ester in the Earth's upper atmosphere (20–50 km). Calculations have also been carried out to determine the ionization energies and fine structure of the lowest ionic state of isobutyl acetate and are compared with a photoelectron spectrum (from 9.5 to 16.7 eV), recorded for the first time. Vibrational structure is observed in the first photoelectron band of this molecule.

1 Introduction

The atmospheric degradation of commonly used volatile organic compounds (VOC) has been of great interest due to their contribution to the greenhouse effect and acid-rain chemistry. Many such compounds are also known to be formed in the atmosphere due to radical reactions with other compounds that are being released into the atmosphere due to industrial activity. Many of these species have also been detected in interstellar space where they may play a role in the complex astrochemistry leading to formation of prebiotic molecules, the origins of life. Investigation of their electronic structure is also significant, since many of them were already reported to be present in interstellar space with VUV photoabsorption spectra serving as fingerprint for their detection. It is therefore important to characterise their electronic states since these

underpin the photochemistry and dissociation dynamics of these species in these environments.

The importance of isobutyl acetate, and thus its main contribution to the atmosphere through human activities, lies in its industrial application as a solvent for the production of various coatings, cosmetic production as a fragrance carrier and as a process solvent in pharmaceuticals. Although commonly used, there is practically no data available on the spectroscopy of this compound in the literature.

Here we report for the first time a high resolution VUV photoabsorption spectrum of isobutyl acetate with absolute cross sections, accompanied by a photoelectron spectrum (PES) and ab initio calculations on the vertical excitation energies and oscillator strengths of the electronic transitions. Measurement and analysis of the photoelectron spectrum aided the assignment of possible Rydberg transitions in the VUV photoabsorption spectrum. For the first time it was possible to resolve and assign vibronic structure in the first ionic PES band of such a chemical compound. The only previous studies of this molecule

^{*} Contribution to the Topical Issue: “Dynamics of Systems at the Nanoscale”, edited by Andrey Solov'yov and Andrei Korol.

^a e-mail: smialek@pg.gda.pl

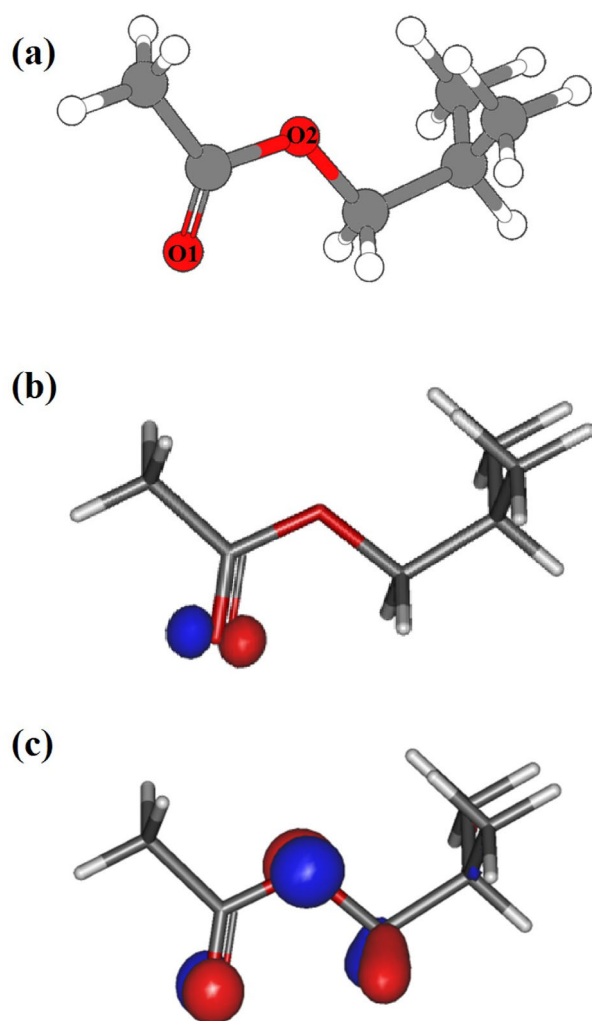


Fig. 1. (a) Structure and numbering of oxygen atoms of the most stable conformer (C_S symmetry) of isobutyl acetate; oxygen atoms in red, carbon in grey and hydrogen in white colour; together with localization of HOMO (b) and HOMO-1 (c) bonding orbitals.

concern its first ionization energy [1]. The absolute photoabsorption cross sections of isobutyl acetate presented here are needed for modeling studies of the Earth's atmosphere and radiation-induced chemistry of esters, and together with the results on previously analysed members of this class: methyl formate [2], ethyl formate [3], isobutyl formate [4] and ethyl acetate [5], help to understand the chemistry of esters and their electronic state spectroscopies.

2 Structure of isobutyl acetate

In the most stable form in the gas phase, isobutyl acetate, $C_6H_{12}O_2$, has C_S symmetry (Fig. 1a). According to our calculations, the electron configuration of the \tilde{X}^1A' ground state is as follows: (a) core orbitals

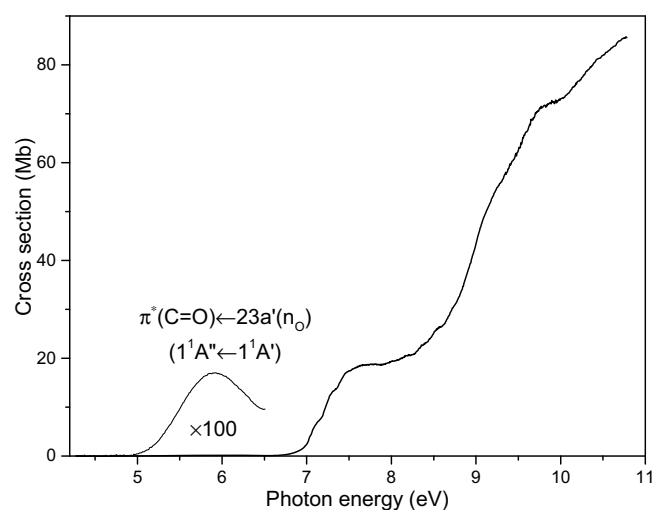


Fig. 2. High resolution photoabsorption spectrum of isobutyl acetate; close-up shows the first valence transition, LUMO $\pi^* \leftarrow n_O(23a')$, recorded over the 4.3–6.5 eV range.

($1a'$)² ($2a'$)² ($3a'$)² ($4a'$)² ($5a'$)² ($6a'$)² ($1a''$)² ($7a'$)² and (b) valence orbitals ($8a'$)² ($9a'$)² ($10a'$)² ($11a'$)² ($12a'$)² ($2a''$)² ($13a'$)² ($14a'$)² ($15a'$)² ($3a''$)² ($16a'$)² ($17a'$)² ($4a''$)² ($18a'$)² ($19a'$)² ($5a''$)² ($20a'$)² ($6a''$)² ($7a''$)² ($21a'$)² ($8a''$)² ($22a'$)² ($9a''$)² ($23a'$)².

The highest occupied molecular orbital (HOMO, $23a'$), shown in Figure 1b, in the neutral ground state is localized predominantly on the terminal oxygen in-plane lone pair (n_{O1}). The second highest occupied molecular orbital (HOMO-1, $9a''$) shows a main contribution on the oxygen out-of-plane lone pair (n_{O2}), Figure 1c. The lowest unoccupied molecular orbital (LUMO) is mainly of π^* antibonding character and it is localized on the C=O bond.

3 Experimental

3.1 Isobutyl acetate sample

The liquid sample used both in the VUV photoabsorption measurements and the PES experiment was purchased from Sigma-Aldrich with a purity of 99%. The sample was degassed by repeated freeze-pump-thaw cycles with no further purification of the sample.

3.2 VUV photoabsorption

The high-resolution VUV photoabsorption spectrum of isobutyl acetate (Fig. 2) was measured at the UV1 beam line of the ASTRID synchrotron facility at Aarhus University, Denmark. The experimental setup has been described in detail previously [6]. Briefly, monochromatised synchrotron radiation passes through a static gas sample and a photomultiplier is used to measure the transmitted light intensity. The incident wavelength is selected using a toroidal dispersion grating with 2000 lines/mm providing a resolution of ~ 0.075 nm (FWHM). The minimum

and maximum wavelengths between which scans are performed, 115–320 nm (10.8–3.9 eV), are determined by the cut-offs of the windows of the gas cell (LiF entrance and MgF₂ exit) and the grating respectively.

The sample pressure is measured using a capacitance manometer (Baratron). In order to ensure that the data were free of any saturation effects [7,8], the cross-section was measured at an appropriate pressure in the range 0.03–1.3 mbar, with typical attenuations <40%. By limiting the absorbance to <40% we avoided both absorption flattening (when the transmitted intensity is very low), and poorly defined (and hence noisy) spectra when the transmitted intensity is high but close to the incident intensity. The synchrotron beam current is monitored throughout the collection of each spectrum and a background scan is recorded for an empty cell. Absolute photoabsorption cross sections are calculated using the Beer-Lambert attenuation law

$$I_t = I_0 \exp(-n\sigma x), \quad (1)$$

where I_t is the radiation intensity transmitted through the gas sample, I_0 is that through the evacuated cell, n is the molecular number density of the sample gas, σ is the absolute photoabsorption cross section, and x is the absorption path length (15.5 cm). The accuracy of the cross section is estimated to be better than $\pm 5\%$ but it should be noted that for low values of the absorption ($I_0 \approx I_t$), the uncertainty increases as a percentage of the measured cross-section. However we estimate the lowest cross section peak of isobutyl acetate (about 0.17 Mb near 5.92 eV) to have an uncertainty of less than 15%, which still amounts to only 0.03 Mb.

3.3 Photoelectron spectroscopy

A He(I) (21.22 eV) photoelectron spectrum of isobutyl acetate was measured at the Université de Liège, Belgium and is shown in Figure 3. The apparatus has also been described previously in detail [9]. Briefly, it consists of a 180° hemispherical electrostatic analyser with a mean radius of 5 cm. The analyser is used in the constant pass energy mode. The incident photons are produced by a d.c. discharge in a two-stage differentially pumped lamp. The energy scale is calibrated using the $X^2\Sigma_g^+$, $\nu' = 0$ and $A^2\Pi_u$, $\nu' = 0$ peaks of N₂⁺, rounded to three decimal places [10,11]. The resolution of the present spectrum is 55 meV and the accuracy of the energy scale is estimated to be ± 2 meV. The photoelectron spectrum presented in this paper is the sum of 125 individual spectra. This procedure allowed a good signal-to-noise ratio while keeping the pressure in the spectrometer low ($< 5 \times 10^{-6}$ mbar), thus minimizing the occurrence of dimers.

4 Computational methods

The theoretical methods used have been discussed in detail in our previous papers [3–5,12], and hence require

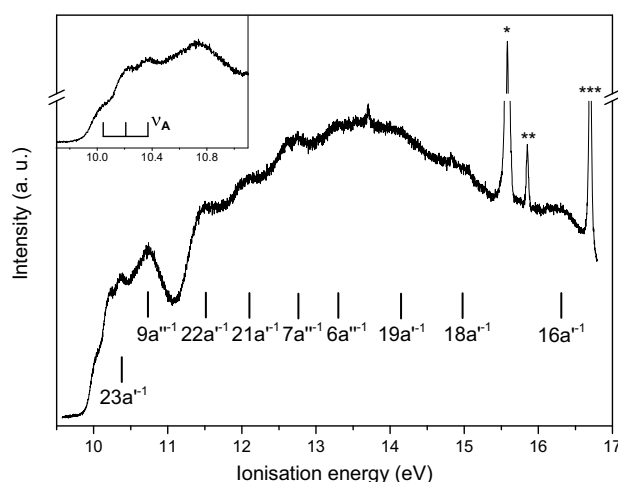


Fig. 3. He(I) photoelectron spectrum of isobutyl acetate, C₆H₁₂O₂, in the 9.5–16.7 eV region (*N₂⁺ X²Σ_g⁺, $\nu' = 0$ produced by the He(I)α line; **N₂⁺ X²Σ_g⁺, $\nu' = 1$ produced by the He(I)α line; ***N₂⁺ A²Π_u, $\nu' = 0$ produced by the He(I) α line); close-up shows the vibronic excitation assignment in the first band.

only a brief mention here. All the calculations were performed applying several post Hartree-Fock ab initio quantum chemistry approaches. The results of the quantum chemical calculations complete the experimental assignment of the required spectra.

The geometries of isobutyl acetate and the corresponding cation were fully optimized when needed. The ground state geometry and harmonic vibrational frequencies of the neutral singlet state (S_0) and ionic doublet state (D_0) of isobutyl acetate were obtained with use of the Gaussian 09 program [13] by means of second-order Møller-Plesset perturbation theory (MP2) calculations in association with the highly accurate aug-cc-pVTZ basis set. The ionic state was described by open-shell unrestricted calculations. Both vertical and adiabatic ionization energies (IEs) of isobutyl acetate were calculated. The first ionization energies were computed from the energy difference between the neutral and ionic ground states. The vertical IE was calculated at the ground state geometry of the neutral compound and the adiabatic IE was evaluated using the optimized geometries of the neutral and ionic ground states. Additionally, the first and second ionization energies were calculated with the coupled-cluster singles and doubles (CCSD), and the coupled-cluster singles, doubles and perturbative triples (CCSD(T)) methods, employing the optimized geometries at the MP2/aug-cc-pVTZ level of approximation. Furthermore, the zero point vibrational energy (ZPVE) corrections to the adiabatic IEs were determined from the MP2/aug-cc-pVTZ harmonic vibrational frequencies. This correction was also applied to the values calculated with the CCSD and CCSD(T) methods. Higher IEs were obtained with the Partial Third Order (P3) and Outer Valence Green's Function (OVGF) propagator methods using the aug-cc-pVTZ basis set and the MP2/aug-cc-pVTZ geometry.

Table 1. Calculated vertical/adiabatic ionization energies of isobutyl acetate (C_S symmetry) at the MP2/aug-cc-pVTZ geometry, compared with experimental values, all in eV. Adiabatic ionization energies include ZPVE correction of -0.0339 eV.

Configuration	Calculated/eV					Experimental/eV
	P3	OVSF	MP2	CCSD	CCSD(T)	
$^2a'$ ($23a'^{-1}$)	10.588	10.778	10.845/10.336	10.992/9.867	11.035/9.969	10.370/10.044
$^2a''$ ($9a''^{-1}$)	11.192	11.262	–	–	–	10.73
$^2a'$ ($22a'^{-1}$)	11.894	11.896	–	–	–	11.51
$^2a''$ ($8a''^{-1}$)	12.024	12.036	–	–	–	–
$^2a'$ ($21a'^{-1}$)	12.044	12.146	–	–	–	12.10
$^2a''$ ($7a''^{-1}$)	13.006	13.107	–	–	–	12.76
$^2a''$ ($6a''^{-1}$)	13.599	13.753	–	–	–	13.30
$^2a'$ ($20a'^{-1}$)	13.418	13.484	–	–	–	–
$^2a''$ ($5a''^{-1}$)	14.027	14.104	–	–	–	–
$^2a'$ ($19a'^{-1}$)	14.472	14.506	–	–	–	14.15
$^2a'$ ($18a'^{-1}$)	15.055	15.044	–	–	–	14.98
$^2a''$ ($4a''^{-1}$)	15.420	15.382	–	–	–	–
$^2a'$ ($17a'^{-1}$)	15.453	15.447	–	–	–	–
$^2a'$ ($16a'^{-1}$)	16.323	16.279	–	–	–	16.31
$^2a''$ ($3a''^{-1}$)	16.682	16.689	–	–	–	–
$^2a'$ ($15a'^{-1}$)	16.990	16.987	–	–	–	–
$^2a'$ ($14a'^{-1}$)	18.555	18.679	–	–	–	–

Finally, the vertical excitation energies, oscillator strengths (f_L , in the length gauge) and radial spatial extents ($\langle r^2 \rangle$) of electronic density of isobutyl acetate have been computed for singlet states with the equation of motion coupled cluster method including single and double excitations (EOM-CCSD). The EOM-CCSD method is well suited to the objectives of our study, since it combines high accuracy with acceptable computational costs, allowing us to use fairly large basis sets.

The optimized geometry of isobutyl acetate at the MP2/aug-cc-pVTZ level of theory has been used in these calculations. However, since many excited states involve significant contributions from diffuse Rydberg orbitals for the purpose of simplifying of the calculations, the aug-cc-pVDZ basis set with additional set of diffuse functions ($6s$, $6p$, $4d$) taken from Kaufmann et al. [14] and localized on the central oxygen atom (O1) was added. Such a basis, designated as aug-cc-pVDZ+R, is generally adequate for description of both valence and Rydberg excited states [3–5]. All EOM-CCSD calculations has been performed with the MOLPRO code [12,15].

5 Results and discussion

5.1 He(I) photoelectron spectrum

The He(I) photoelectron spectrum of isobutyl acetate over the energy range 9.5–16.7 eV is shown in Figure 3. The calculated vertical and adiabatic ionization energies, obtained for the C_S symmetry of this molecule through various calculation methods, as well as those determined based on the present experimental spectrum, are shown in Table 1. The lowest vertical (10.370 eV) and adiabatic (10.044 eV) values of IEs obtained from the spectra

Table 2. Energy positions and vibrational analysis of vibrational features observed in the first photoelectron band ($23a'^{-1}$) of isobutyl acetate.

Peak energy/eV	Assignment	ΔE (ν_A)/eV
10.044	Adiabatic IE	–
10.208	$1\nu_A$	0.164
10.370	$2\nu_A$	0.162

agree well with the values obtained from P3 calculations (10.588 eV for the vertical value). The experimental results are also in a sensible agreement with calculations using the CCSD method (10.992 and 9.867 eV, respectively). The calculations predict the adiabatic value with a deviation from experiment of about 0.05 eV, which is in agreement with the results obtained previously for ethyl formate [3], isobutyl formate [4] and ethyl acetate [5]. The vertical value for this state agrees well with the only value available in the literature obtained by Watanabe et al., yielding 9.97 eV [1]. Similar results were obtained for other ester molecules analysed previously [2–5]. It is worth noticing that the order of some molecular orbitals is inverted in the calculations with respect to the determined electron configuration of the molecule in its ground state, just like in case of previously reported results obtained for other ester molecules.

In Figure 3 (inset), the low energy part of the photoelectron spectrum is shown with the $23a'^{-1}$ state showing a vibrational structure, which is assigned in Table 2. With an average spacing of 0.163 eV it has been denoted as a progression of ν_A mode, which as for all ester molecules analysed previously, corresponds to a combination of C–O stretch combined with C=O stretch.

Table 3. Calculated vertical excitation energies (EOM-CCSD/aug-cc-pVDZ+R) (in eV) and oscillator strengths for the first 24 states of isobutyl acetate compared with the present experimental vertical energies and VUV absorption cross sections.

State	E/eV	f_L	$\langle r^2 \rangle$	Main character	E_{exp}/eV	Cross section/Mb
A''	5.976	0.00097	114	23 a' (n_{O1}) \rightarrow LUMO $\pi^*(\text{C=O})$	5.918	0.17
a'	7.297	0.02996	154	23 a' \rightarrow 3s σ	7.033	3.82
A''	7.948	0.01414	151	9 A'' \rightarrow 3s σ	7.755	18.86
a'	8.050	0.01453	176	23 a' \rightarrow 3p σ	7.653	18.63
A''	8.078	0.00001	180	23 a' \rightarrow 3p π	–	–
a'	8.259	0.16277	144	9 A'' \rightarrow LUMO $\pi^*(\text{C=O})$	7.669	18.60
a'	8.340	0.00971	201	23 a' \rightarrow 3p σ'	7.814	18.76
A''	8.499	0.01639	171	9 A'' \rightarrow 3p σ	8.197	20.51
a'	8.575	0.01679	228	23 a' \rightarrow 3d σ	8.366	22.64
a'	8.679	0.00649	177	9 A'' \rightarrow 3p π	–	–
A''	8.806	0.00240	238	23 a' \rightarrow 3d π	–	–
A''	8.810	0.00636	187	9 A'' \rightarrow 3p σ'	–	–
a'	8.815	0.00232	240	23 a' \rightarrow 3d σ'	–	–
a'	8.834	0.01264	257	23 a' \rightarrow 3d σ''	8.394	22.90
a'	8.852	0.04610	165	22 a' \rightarrow 3s σ	8.539	25.86
A''	8.882	0.00137	251	23 a' \rightarrow 3d π'	–	–
a'	8.945	0.01121	323	23 a' \rightarrow 4s σ	8.667	28.47
a'	9.025	0.00896	179	21 a' \rightarrow 3s σ	8.725	30.25
A''	9.084	0.03368	193	8 A'' \rightarrow 3s σ	9.116	49.80
A''	9.133	<0.00001	438	23 a' \rightarrow 4p π	–	–
a'	9.151	0.00137	441	23 a' \rightarrow 4p σ	–	–
A''	9.169	0.00369	227	9 A'' \rightarrow 3d σ	–	–
a'	9.254	0.00091	497	23 a' \rightarrow 4d σ	–	–
a'	9.283	0.00920	224	22 a' \rightarrow 3p σ	9.778	71.22

5.2 Valence states and transitions and the Rydberg series of isobutyl acetate

The first 24 states of isobutyl acetate were calculated (Tab. 3) allowing assignment of the absorption band centred at 5.918 eV to ($\pi^*(\text{C=O}) \leftarrow n_{O1}(23a')$) transition and the one centred at 7.669 eV to the ($\pi^*(\text{C=O}) \leftarrow n_{O2}(9a'')$) transition (Figs. 2 and 4).

The first band, shown in Figure 2, with a maximum cross section of 0.17 Mb, has been identified as the transition from the terminal oxygen in-plane lone pair (n_{O1}) to the first π antibonding molecular orbital ($\pi^*(\text{C=O}) \leftarrow n_{O1}(23a')$) ($1^1a'' \leftarrow 1^1a'$). The calculated value of the oscillator strength, ca. 1×10^{-3} , is comparable with the values obtained for the previously analysed esters [2–5]. No vibronic structure has been resolved on this band, which is not surprising since the electronic transition is from a non-bonding electron.

It was possible to assign some vibrational progressions in the 7.0–8.75 eV range over the bands identified as pure Rydberg transitions and the details of these assignments are shown in Figure 4, and are also listed in Table 4. The most pronounced series over the structure, centred at 7.669 eV with a cross section of 18.6 Mb from the $\pi^*(\text{C=O}) \leftarrow n_{O2}(9a'')$ transition, is proposed to be due to the ν'_A mode (C–O and C=O stretches) with an average spacing of 0.182 eV, and one quantum of the ν'_B mode (OCC deformation combined with CO stretch and CH_3

Table 4. Proposed vibrational assignments in the 7.0–8.75 eV absorption bands of isobutyl acetate, $\text{C}_6\text{H}_{12}\text{O}_2$.

Energy/eV	Assignment	$\Delta E(\nu'_B)/\text{eV}$	$\Delta E(\nu'_A)/\text{eV}$
Second band: $\pi^*(\text{C=O}) \leftarrow n_{O1}(23a')$			
7.031	ν_{00}	–	–
7.086	$1\nu'_B$	–	0.055
7.218	$1\nu'_A$	0.194	–
7.280	$1\nu'_A + 1\nu'_B$	–	0.062
7.395	$2\nu'_A$	0.184	–
7.464	$2\nu'_A + 1\nu'_B$	–	0.069
8.006	ν_{00}	0.176	–
8.186	$1\nu'_A$	0.180	–
8.357	$2\nu'_A$	0.171	–
8.544	$3\nu'_A$	0.187	–
8.544	$4\nu'_A$	0.178	–

rocking), spaced on average by 0.062 eV. This progression has also been observed in the case of all previously measured esters.

The band from the $\pi^*(\text{C=O}) \leftarrow n_{O2}(9a'')$ transition has an oscillator strength of 0.16 according to the calculations, thus being the most pronounced feature in the measured spectrum.

The photoabsorption spectrum above 7.5 eV shows a number of superimposed structures extending

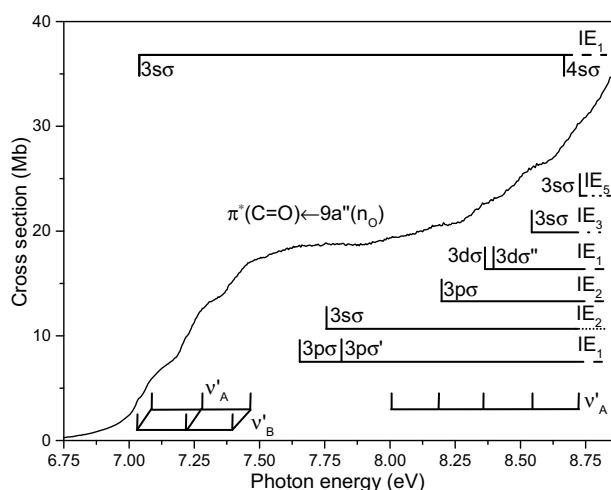


Fig. 4. High resolution photoabsorption spectrum of isobutyl acetate over the 6.75–8.85 eV range.

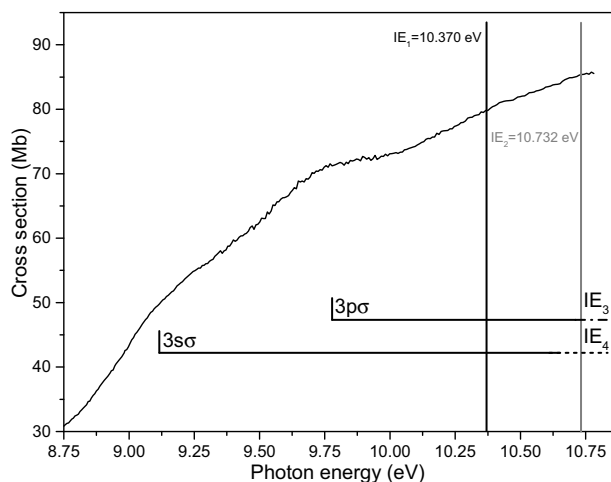


Fig. 5. High resolution photoabsorption spectrum of isobutyl acetate over the 8.75–10.75 eV range; dashed line indicates a tentative assignment.

to the lowest ionization energy. The Rydberg transitions that were possible to be identified are labeled in Figures 4 and 5 and presented in Table 5 and originate mainly from the HOMO ($23a'$) according to our calculations. The positions of the peaks, E_n , have been predicted using the well-known Rydberg formula: $E_n = E_i - R/(n - \delta)^2$, where E_i is the ionization energy, R is the Rydberg constant 13.61 eV, n is the principal quantum number of the Rydberg orbital of energy E_n , and δ is the quantum defect. Quantum defects are expected to be in range of 1.0–0.9, 0.6–0.3 and <0.25 for ns , np and nd series, respectively. The ionization energy used in this assessment was the adiabatic value for $23a'^{-1}$, i.e. 10.044 eV, whereas for $8a''^{-1}$ a calculated value of 12.03 eV was employed. In the measured experimental spectrum due to a massive overlap of electronic states that occurs already at low energy, it was not possible to assign the transitions unambiguously; thus only the lower members, mainly of

Table 5. Energies (in eV), quantum defects and assignments of the ns , np and nd Rydberg series converging to the first five ionic electronic ground state of isobutyl acetate.

Vertical transition energy/eV	Quantum defect, δ	Assignment
$IE_1 = 10.044$ eV		
7.033	0.87	$3s\sigma$
8.667	0.86	$4s\sigma$
7.653	0.61	$3p\sigma$
7.814	0.53	$3p\sigma'$
8.366	0.15	$3d\sigma$
8.394	0.13	$3d\sigma'$
$IE_2 = 10.73$ eV		
7.755	0.86	$3s\sigma$
$IE_3 = 11.51$ eV		
8.539	0.86	$3s\sigma$
9.283	0.53	$3p\sigma$
$IE_4 = 12.03$ eV*		
9.116	0.97	$3s\sigma$
$IE_5 = 12.10$ eV		
8.725	0.99	$3s\sigma$

the ns series, converging to $23a'^{-1}$, $9a''^{-1}$, $22a'^{-1}$, $8a''^{-1}$ and $21a'^{-1}$ states were assigned.

The feature at 7.033 eV was assigned to the ($3s\sigma \leftarrow n_{O1}$, $23a'$) Rydberg transition with a quantum defect of 0.87 (Tab. 5). The calculated value of 7.297 eV is in a good agreement with the one found experimentally. Another member of this series, $4s\sigma$, was assigned at 8.667 eV with quantum defect of 0.86, and was also found to be in a good agreement with the calculated value of 8.945 eV. The first members of $np\sigma$ and $np\sigma'$ series were found at 7.653 eV and 7.814 eV with quantum defects of 0.61 and 0.53, respectively (Tab. 5). Calculated energies for these transitions (Tab. 3), yielding 8.050 eV and 8.340 eV, agree with experimental values reasonably well particularly when the possible valence character of these transitions is also accounted for. The features at 8.366 eV and 8.394 eV were assigned to first transitions of the $nd\sigma$ and $nd\sigma''$, respectively, with corresponding values of quantum defects $\delta = 0.15$ and $\delta = 0.13$. These are also in agreement with the calculated values of 8.575 eV and 8.834 eV.

The first members of ns Rydberg series converging to $9a''^{-1}$, $22a'^{-1}$, $8a''^{-1}$ and $21a'^{-1}$ states were assigned at 7.755, 8.539, 9.116 and 8.725 eV with quantum defects of 0.86, 0.86, 0.97 and 0.99, respectively. The assigned values agree reasonably well with the values obtained from calculations. Due to a continuous overlap of Rydberg transitions at higher energies and lack of visible structures in the spectrum, no attempt was made to assign higher members of these series.

5.3 Absolute photoabsorption cross-sections and atmospheric photolysis

Since isobutyl acetate is widely used in industry, and thus is of environmental importance, it is worth estimating the photolysis rates for this compound. Here we present the absolute photoabsorption cross sections of isobutyl

acetate that in combination with solar actinic flux [16] measurements from the literature can be used for this purpose. The photolysis rates of this compound in the atmosphere from an altitude close to the ground to the stratopause at 50 km can therefore be calculated. Details of the program used to perform the calculations have been given previously [17]. The quantum yield for dissociation following absorption is assumed to be unity. The reciprocal of the photolysis rate at a given altitude corresponds to the local photolysis lifetime. Photolysis lifetimes of ca. 270 days and photolysis rates of $4.27 \times 10^{-8} \text{ s}^{-1}$ were calculated at altitudes around 22 km, indicating the high stability of this molecule to photodissociation. Even at higher altitudes of about 45 km, the lifetime of this molecule is predicted to be over 26 h and leads to rather low values of photolysis rates of $1.05 \times 10^{-5} \text{ s}^{-1}$. Therefore, since isobutyl acetate cannot be broken up efficiently by VUV absorption it is important to assess other possible pathways as a sink mechanism of this molecule from the atmosphere.

Rate constants for gas-phase reactions of OH [18] and Cl [19,20] radicals with isobutyl acetate have been measured, yielding, for reactions at room temperature, $(9.97 \pm 0.60) \times 10^{-11}$ and $(6.33 \pm 0.52) \times 10^{-12}$, in $\text{cm}^3 \text{ molecule}^{-1} \text{ s}^{-1}$, respectively. These cases prove that not only is radical attack the main mechanism for this ester removal from the atmosphere and is equally probable for both types of radicals, but also that the UV photolysis is not expected to play a significant role in the removal process.

6 Conclusions

We present for the first time the complete electronic spectra of isobutyl acetate together with absolute photoabsorption cross sections from 4.5 to 10.7 eV. The structures observed in the spectrum were assigned to both valence and Rydberg transitions, based on ab initio calculations of vertical excitation energies and oscillator strengths of this molecule. Fine structure has been assigned to vibrational series involving predominantly excitations of ν'_A and ν'_B modes that are due to C–O and C=O stretches and OCC deformation combined with CO stretch and CH₃ rocking, respectively. In the He(I) photoelectron spectrum of isobutyl acetate, vibrational excitations in the first ionic state were resolved and also assigned to the ν_A mode. The theoretical calculations presented here are in a good agreement with experimental data. Based on the photoabsorption cross section, photolysis lifetimes of isobutyl acetate have been calculated for the Earth's troposphere and stratosphere and based on the literature values of rate constants for the reactions of isobutyl acetate with hydroxyl and chlorine radicals, photolysis was excluded as a significant process of removal of this compound from the atmosphere. The data presented here are in good agreement with the results reported previously for other esters.

M.A.Ś. acknowledges the visiting fellow position in the Molecular Physics Group, Open University. P.L.V. acknowledges the Portuguese National Funding Agency (FCT-MCTES) through

UID/FIS/00068/2013 grant. The authors wish to acknowledge the beam time at the ASTRID synchrotron at Aarhus University, Denmark, supported by the European Union (EU) I3 programme ELISA, Grant Agreement No. 226716. We also acknowledge the financial support provided by the European Commission through the Access to Research Infrastructure action of the Improving Human Potential Programme. M.L. is thankful to the 7th Framework Programme of the European Union (grant agreement No. 321971). All calculations have been performed at the Academic Computer Centre (CI TASK) in Gdańsk and using resources provided by Wrocław Centre for Networking and Supercomputing (WCSS).

Author contribution statement

MAŚ performed the PA measurements, PES processing, all data analysis and wrote the manuscript; ML performed and analyzed all necessary calculations and wrote the 'Computational methods' section; M-J H-F and JD performed PES measurements; SVH and NCJ performed PA measurements, data processing and edited the manuscript; NJM edited the manuscript; PLV edited the manuscript and contributed to the photolysis rate calculations.

Open Access This is an open access article distributed under the terms of the Creative Commons Attribution License (<http://creativecommons.org/licenses/by/4.0>), which permits unrestricted use, distribution, and reproduction in any medium, provided the original work is properly cited.

References

1. K. Watanabe, T. Nakayama, J. Mottl, J. Quant. Spectrosc. Radiat. Transf. **2**, 369 (1962)
2. Y. Nunes, G. Martins, N.J. Mason, D. Duflot, S.V. Hoffmann, J. Delwiche, M.J. Hubin-Franskin, P. Limão-Vieira, Phys. Chem. Chem. Phys. **12**, 15734 (2010)
3. M.A. Śmiałek, M. Łabuda, J. Guthmuller, M.J. Hubin-Franskin, J. Delwiche, D. Duflot, N.J. Mason, S.V. Hoffmann, N.C. Jones, P. Limão-Vieira, J. Chem. Phys. **141**, 104311 (2014)
4. M.A. Śmiałek, M. Łabuda, J. Guthmuller, S.V. Hoffmann, N.C. Jones, M.A. MacDonald, L. Zuin, N.J. Mason, P. Limão-Vieira, J. Chem. Phys. A **119**, 8647 (2015)
5. M.A. Śmiałek, M. Łabuda, J. Guthmuller, M.J. Hubin-Franskin, J. Delwiche, S.V. Hoffmann, N.C. Jones, N.J. Mason, P. Limão-Vieira, Eur. Phys. J. D **70**, 138 (2016)
6. S. Eden, P. Limão-Vieira, S. Hoffmann, N. Mason, Chem. Phys. **323**, 313 (2006)
7. N. Mason, J. Gingell, J. Davies, H. Zhao, I. Walker, M. Siggel, J. Phys. B: At. Mol. Opt. Phys. **29**, 3075 (1996)
8. W.F. Chan, G. Cooper, C.E. Brion, Phys. Rev. A **44**, 186 (1991)
9. J. Delwiche, P. Natalis, J. Momigny, J.E. Collin, J. Electron Spectrosc. Relat. Phenom. **1**, 219 (1972–1973)
10. K.P. Huber, C. Jungen, J. Chem. Phys. **92**, 850 (1990)
11. D.A. Shaw, D.M.P. Holland, M.A. MacDonald, A. Hopkirk, M.A. Hayes, S.M. McSweeney, Chem. Phys. **166**, 379 (1992)

12. M. Labuda, J. Guthmuller, Eur. Phys. J. Spec. Top. **222**, 2257 (2013)
13. M.J. Frisch, G.W. Trucks, H.B. Schlegel, G.E. Scuseria, M.A. Robb, J.R. Cheeseman, G. Scalmani, V. Barone, B. Mennucci, G.A. Petersson et al., *Gaussian 09 Revision B.1* (Gaussian Inc., Wallingford, CT, 2009)
14. K. Kaufmann, W. Baumeister, M. Jungen, J. Phys. B: At. Mol. Opt. Phys. **22**, 2223 (1989)
15. H.J. Werner, P.J. Knowles, G. Knizia, F.R. Manby, M. Schütz, P. Celani, T. Korona, R. Lindh, A. Mitrushenkov, G. Rauhut et al., *Molpro, version 2012.1, a package of ab initio programs* (2012), <http://www.molpro.net>
16. W.B. DeMore, S.P. Sander, D.M. Golden, R.F. Hampson, M.J. Kurylo, C.J. Howard, A.R. Ravishankara, C.E. Kolb, M.J. Molina, *Chemical kinetics and photochemical data for use in stratospheric modeling, evaluation number 12* (1997)
17. P. Limão Vieira, S. Eden, P. Kendall, N. Mason, S. Hoffmann, Chem. Phys. Lett. **364**, 535 (2002)
18. S. Le Calve, G. Le Bras, A. Mellouki, Int. J. Chem. Kinet. **29**, 683 (1997)
19. A. Notario, G.L. Bras, A. Mellouki, J. Phys. Chem. A **102**, 3112 (1998)
20. J.H. Xing, K. Takahashi, M.D. Hurley, T.J. Wallington, Chem. Phys. Lett. **474**, 268 (2009)

